Retraction

Retracted: Analysis of Influencing Factors of PM2.5 Concentration and Design of a Pollutant Diffusion Model Based on an Artificial Neural Network in the Environment of the Internet of Vehicles

Computational Intelligence and Neuroscience

This article has been retracted by Hindawi following an investigation undertaken by the publisher [1]. This investigation has uncovered evidence of one or more of the following indicators of systematic manipulation of the publication process:

(1) Discrepancies in scope

(2) Discrepancies in the description of the research reported

(3) Discrepancies between the availability of data and the research described

(4) Inappropriate citations

(5) Incoherent, meaningless and/or irrelevant content included in the article

(6) Peer-review manipulation

The presence of these indicators undermines our confidence in the integrity of the article's content and we cannot, therefore, vouch for its reliability. Please note that this notice is intended solely to alert readers that the content of this article is unreliable. We have not investigated whether authors were aware of or involved in the systematic manipulation of the publication process.

Wiley and Hindawi regrets that the usual quality checks did not identify these issues before publication and have since put additional measures in place to safeguard research integrity.

We wish to credit our own Research Integrity and Research Publishing teams and anonymous and named external researchers and research integrity experts for contributing to this investigation.

The corresponding author, as the representative of all authors, has been given the opportunity to register their agreement or disagreement to this retraction. We have kept a record of any response received.

References

[1] S. Li, X. Pan, and Q. Li, "Analysis of Influencing Factors of PM2.5 Concentration and Design of a Pollutant Diffusion Model Based on an Artificial Neural Network in the Environment of the Internet of Vehicles," *Computational Intelligence and Neuroscience*, vol. 2021, Article ID 3092197, 15 pages, 2021.

Research Article

Analysis of Influencing Factors of PM2.5 Concentration and Design of a Pollutant Diffusion Model Based on an Artificial Neural Network in the Environment of the Internet of Vehicles

Sumin Li , Xiuqin Pan , and Qian Li

School of Information Engineering, Minzu University of China, Beijing 100081, China

Correspondence should be addressed to Sumin Li; suminli@muc.edu.cn

With the development of the automobile industry, artificial intelligence, big data, 5G, and other technologies, the Internet of Vehicles (IoV) industry has entered a stage of rapid development. In this paper, a pollutant diffusion model based on an artificial neural network is designed in the context of a vehicle network. The application of artificial neural networks in haze prediction is studied. This paper first analyzes the causes and influencing factors of haze and selects the most representative and relatively large meteorological factors from temperature, wind, relative humidity, and several pollutant factors. Through training and simulation, a haze prediction model in the Beijing, Tianjin, and Hebei regions of China is established. Finally, according to the collected meteorological data, the pollutant diffusion model is established. The model is deduced by a standard mathematical formula, which makes the prediction results more accurate and rigorous, and the main conclusions and feasible scientific suggestions are obtained. The simulation results show that the method is effective. By strengthening the service system of the IoV, meteorological services can be more intelligent, and the information acquisition and service ability of the vehicle network can be effectively improved.

1. Introduction

Currently, the safety protection function and measures of the vehicle network industry are not perfect, and the related technologies are also in the process of continuous exploration [1, 2]. There is still tremendous room for further improvement for the deepening service of comprehensive scenarios such as humans, vehicles, roads, facilities, and networks. As an important factor affecting car driving, the weather has a profound impact on the car driving experience and driving safety. Extreme weather, such as rainstorms, waterlogging, snow, road icing, fog, haze, sandstorms, and dazzling sunshine, has different degrees of impact on car driving. This requires accurate weather forecasting capabilities and diversified weather data, as well as customized and diversified intelligent weather solutions to create more value for the IoV services [3, 4]. Due to many uncertainties of climate, it brings great obstacles to the research. In other words, negative radiation means that the energy radiated

outwards is greater than the radiation energy received, which makes the climate cool [5, 6].

In contrast, positive radiation makes the Earth's surface warm [7, 8]. Global warming is an indisputable fact. The main influencing factors are the increase in atmospheric concentrations of greenhouse gases and aerosols, which change the balance of the Earth's radiation budget and eventually lead to climate change, such as the formation of greenhouse effects and haze. The haze data obtained by the monitoring station are point data, and the regional data depend on the data difference technology. Because of the advantages of a wide monitoring range and short cycle, remote sensing technology has become an important tool for large-scale haze monitoring [9, 10]. At present, the research and application of remote sensing technology in haze mainly include aerosol optical thickness, astigmatism coefficient, vertical distribution, haze image removal technology, and so on. Remote sensing monitoring of haze mainly uses remote sensing data to obtain aerosol optical

thickness and other data, analyzes the relationship between aerosol optical thickness and haze concentration, and uses the aerosol optical thickness inversion algorithm [11, 12]. The governance of air pollution is a problem between regions that cannot be dealt with the perspective of a single region, and the joint governance between regions can improve the atmospheric environment of a city. Quality has the effect of improvement. One of the characteristics of current air pollution control is separate regional environmental pollution control. However, it is difficult to achieve the ideal effect if we rely on local air pollution control measures and ignore the transmission characteristics of air pollutants between regions [13, 14]. Therefore, a more effective measure to control air pollution is to adopt the method of regional joint governance, to recognize the multiregional joint mechanism, to reveal the main reasons for the formation of air pollution between regions, and then to develop a feasible and effective air pollution control scheme [15, 16]. Weather scene service in the Internet of Vehicles plays an essential role in the "ecological Internet of Vehicles." It can provide users with weather forecasts, road temperature and humidity, road water and ice data, visibility reminders, and other information, greatly improving the optimization of the car driving experience and ensuring driving safety.

This paper is committed to applying artificial neural networks in the analysis of haze data in the environment of the IoV to make the prediction data more accurate. High-precision and refined meteorological services can realize the early warning of meteorological disaster risks and the IoV and help users take corresponding measures to minimize the possible damage caused by sudden meteorological disasters such as haze. At the same time, it can effectively improve the user experience through targeted and accurate meteorological scene services, which can create more value for IoV services. Artificial neural networks include BP, RBF, SOM, Hopfield, and deep learning [17, 18]. Through the establishment of an artificial neural network model, the haze forecast level can be continuously improved. In this paper, the use of neural networks and deep learning and other cutting-edge technologies, in-depth excavation of the IoV service scenarios, through the creation of professional weather solutions for the IoV, continues to help the development of the IoV.

The contributions of this study include the following:

(i) This paper introduces haze forecasting and considers weather route navigation, the adjustment of temperature, humidity, and air quality in the automatic IoV, the prediction of road temperature and humidity, the prediction and a reminder of visibility, the correlation analysis of temperature, and automatic driving assisted by meteorological information and designs a framework based on the IoV and meteorological factors.

(ii) Artificial neural networks are explored and analyzed, focusing on the principle of artificial neural networks, as well as their learning process, advantages, and disadvantages.

(iii) The pollutant diffusion model is established, and further it is optimized to derive the pollutant concentration at any point in space.

(iv) Based on the relevant meteorological information and pollutant concentration data of monitoring stations in the Beijing-Tianjin-Hebei region, the haze prediction model designed in this paper is tested, and the established model is improved through actual meteorological data training.

The remainder of this paper is organized as follows. Section 2 discusses related works, and the pollutant diffusion model is outlined in Section 3. The analysis and prediction of the PM2.5 concentration are presented in Section 4. Section 5 shows the experimental test results, and Section 6 concludes the paper with a summary and proposes directions for future research.

2. Related Work

With the in-depth application of cloud computing, the Internet of Things, mobile Internet, artificial intelligence, and other new technologies, relying on the progress of meteorological science and technology, intelligent weather with self-perception, judgment, analysis, selection, action, innovation, and adaptive ability can provide more accurate, more reliable, and more intelligent weather forecasts [19, 20]. The IoV "entering" the car can effectively help the driver adjust to the weather, make the best travel decisions, and provide a more accurate warning for drivers on the road [21, 22]. At present, Internet of Vehicles technology is widely used in bad weather environments. Countries worldwide have taken measures to improve driving safety under bad weather conditions. An early warning system of bad weather is realized through the Internet of Things (IoT) technology. The early warning system of bad weather is usually realized through the dynamic message sign (DMS) of roadside terminal and vehicle terminal [23]. It is the infrastructure to display the information sent by the management center in real-time, usually located in front of the often bad weather area. Vehicle terminals always exist to help drivers adjust their driving behavior before entering bad weather areas. The absorption of solar radiation by the Earth's atmosphere at different altitudes is different, resulting in a distinct vertical distribution of the Earth's atmosphere at the vertical altitude. Infrared spectra are an important spectral range for various qualitative and quantitative research and applications. By measuring the infrared absorption spectrum of gases, we can realize the detection and accurate measurement of gases in the atmosphere [24, 25]. The study of the absorption of H_2O, CO_2, and O_3 can better understand the impact of these gases on climate change, atmospheric circulation, and the balance of atmospheric radiation budgets. Due to the different chemical structures of atmospheric absorption gas molecules, their absorption spectra also have their unique properties, and the absorption intensity and line shape are also different under different temperature and pressure environments. Therefore, understanding the basic theory of gas absorption spectra and the calculation method

of transmittance helps develop related research [26, 27]. Since the 1990s, an increasing number of scholars have begun to apply neural networks to detect pollutants and have made major breakthroughs. It is more suitable for modern environmental detection than traditional methods. The characteristics of artificial neural networks determine the feasibility of their combination with haze prediction [28, 29].

At present, statistical forecasts and numerical forecasts are commonly used in the field of air quality prediction. Among them, the United States, Japan, the Netherlands, Canada, and other developed countries are mainly committed to developing numerical forecasts [30, 31]. By analyzing the relationship between haze and aerosols, Zhang et al. pointed out that the main cause of haze is serious aerosol pollution [32]. The mass concentrations of sulfate, organic carbon, nitrate, and carbon in aerosols are much higher than those in Europe, which are closely related to the high emissions of anthropogenic pollution caused by rapid economic development [33–35]. Currently, the neural network method has become a powerful tool for air pollution prediction. Relevant studies show that the prediction model established by artificial neural networks has good objectivity, and it can well capture the inherent law between meteorological elements and air pollution [36, 37]. Its biggest feature is that it does not need to design any mathematical model but completes the whole network through the interaction between neurons network information processing to obtain a good prediction effect. Chen et al. established the air quality index (API) prediction model of Shanghai based on an artificial neural network (ANN). The model is a multilayer perceptual (MLP) network, with meteorological forecast data as the main input to forecast the air quality index (API) of Shanghai on the second day [38]. Currently, the combination of artificial neural networks and haze prediction is still in the exploratory stage.

3. System Framework of Internet of Vehicles and Artificial Neural Network

The IoV uses sensors, video capture devices, intelligent terminals loaded on the vehicle to collect the road, traffic, and other information around the vehicle [39, 40]. Through the transmission network, the collected information is extracted and effectively used on the information network platform. According to the different functional requirements of the users of the IoV, we can effectively supervise the operation status of the IoV and provide users with diversified intelligent services to realize the interconnection between vehicles and roads, vehicles and vehicles, vehicles and owners, and vehicles and social public information platforms. At present, most of the services provided by the IoV are still focused on the intelligent monitoring of vehicles, and the integration of vehicles, people, roads, weather, and public value-added services has not been realized [41, 42]. The IoV system is mainly composed of a terminal layer, network layer, platform layer, and application layer. The system framework is shown in Figure 1.

(1) *Terminal Layer.* Mainly using RFID (radio frequency identification) technology, OBD (on board diagnostic) vehicle intelligent terminals, smartphones, tablet computers, vehicle sensors, and other information, collection devices collect vehicle information such as fuel consumption, mileage, location, road conditions, traffic, and other vehicle surrounding information, as well as driver's driving behavior and other information and transmit them to the information processing layer through the transmission layer [43].

(2) *Network Layer.* This layer mainly uses wired communication networks, wireless communication networks, the Internet, and other transmission means to realize the transmission of effective information collected by the front end of the Internet of Vehicles.

(3) *Platform Layer.* This layer is mainly composed of a server, cloud computing platform, middleware, database, system software, application program, and other software and hardware systems [44, 45]. It completes the storage, control, coding, decoding, encryption, management, statistics, query, and other processing of the Internet of Vehicles information and calls each function module of the information supply layer after processing.

(4) *Application Layer.* For the IoV users, through the application system running on the navigator, mobile phone, and intelligent mobile terminal, the Internet of Vehicles intelligent applications for the Internet of Vehicles users are provided [46]. The application system of the application layer interacts with a remote server and cloud computing platform through wireless and wired transmission network. Generally, it has the functions of GPS positioning, track playback, vehicle status monitoring, vehicle condition analysis, road rescue, mileage statistics, fuel consumption detection, remote diagnosis, vehicle alarm, and remote diagnosis vehicle alarm. Electronic maps and other functions can share information with telecom operators, third-party payment platforms, and urban public resources and provide users with various value-added services.

In addition, smart weather also has great potential in automatic driving. Part of the automatic driving technology adopts the scheme of improving the accuracy of environmental sensors, multisensor combinations, and optimization algorithms and still cannot perceive road changes in the next few hours. The introduction of smart weather can not only effectively solve this problem but also save many costs and escort the development of unmanned driving [32, 47]. In addition to its application in the IoV, smart weather has been applied in tourism, insurance, logistics, agriculture, and other fields. Artificial neural networks, AI fusion numerical models, deep learning, and other modern information technologies have effectively solved the problem of insufficient capacity of traditional meteorological services, greatly
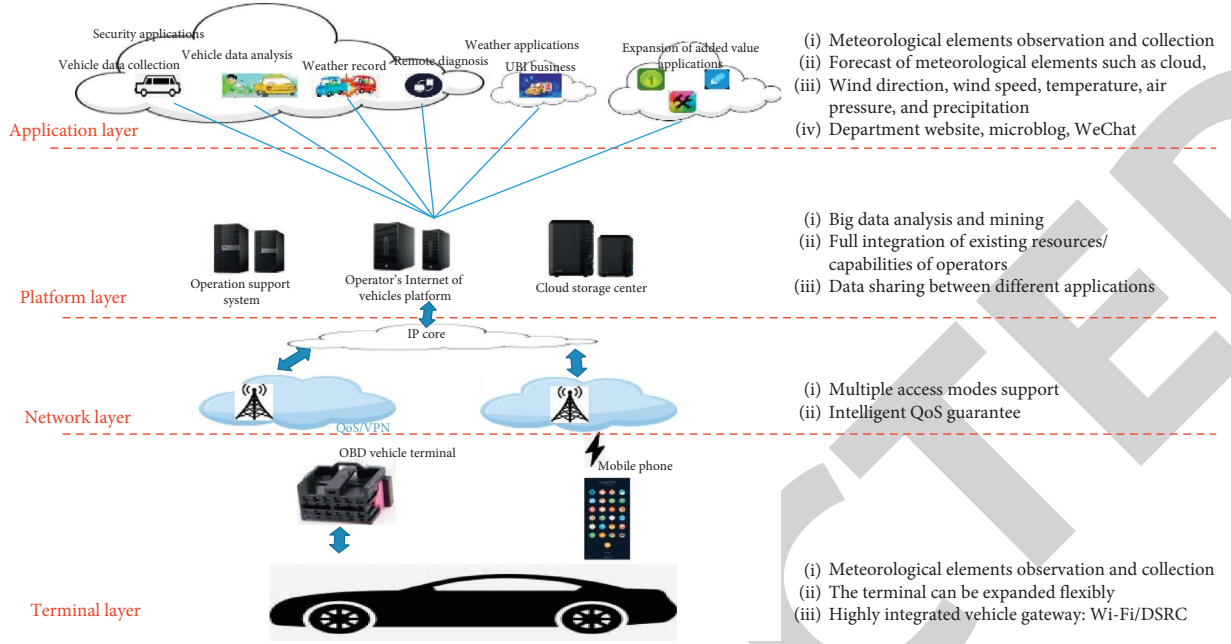
Figure 1: The system framework of the Internet of Vehicles.

improved the efficiency of meteorological services, and promoted the intelligent and high-quality development of various industries. Figure 2 shows the composition structure diagram of the application of artificial neural networks in smart weather and the IoV.

4. Diffusion Model of Air Pollutants

In some wavelength ranges, the absorption coefficient is very large, called the absorption band [28]. The absorption band is composed of many absorption lines. Outside the absorption band, the absorption coefficient is very small or equal to 0 (no absorption). The absorption of gas molecules in the infrared region is mainly caused by the vibrational and rotational energy level transitions between the atoms of the molecules called vibrational and rotational spectroscopy. The spectrum with only rotational energy level transition, called a rotational spectrum, often occurs in the far-infrared and microwave region with a longer wavelength. In contrast, the spectrum with only electronic energy level transition often occurs in the ultraviolet or visible region [15, 48].

Taking a single pollution source as an example, from free diffusion to limited diffusion, the spatial and ground concentration diffusion models of elevated point sources are discussed, and the final pollutant diffusion model is gradually refined from simple to complex.

4.1. Free Diffusion Model of Single Pollution Source. To make the diffusion of pollutants more visual and accurate, this paper uses a Gaussian diffusion model to visualize pollutants' diffusion. Generally, before establishing a model, certain conditions are needed. In the process of diffusion,

assuming that there are no obstacles in the diffusion space of the point source and regardless of the hindrance of diffusion, the diffusion of pollutants is a two-dimensional normal distribution in the Y-axis and Z-axis [16, 49]. The random variables in the coordinate direction are independent, and the distribution density is the product of a one-dimensional normal distribution density function. Based on the assumption of a normal distribution, the distribution function of the concentration at any point downwind from a point source can be obtained by taking $\mu = 0$:

$$C(x, y, z) = A(x)\exp\left[\frac{1}{2}\left(\frac{y^2}{\sigma_y^2} + \frac{z^2}{\sigma_z^2}\right)\right], \tag{1}$$

where $A(x)$ is an unknown parameter function and σ_y and σ_z are the standard deviation of the horizontal and vertical directions, i.e., the diffusion parameters in the y and x directions, and the unit is m.

According to the hypothesis of continuity and conservation, the intensity q of the source flow at the cross section of the x-axis of the pollution source is 0.

$$q = \int_{-\infty}^{+\infty}\int_{-\infty}^{+\infty} uC\,\mathrm{d}y\mathrm{d}z, \tag{2}$$

in which u is the average wind speed.

Combined with formulas (1) and (2) and according to the assumption that the wind speed is stable and considering

$$\int_{-\infty}^{+\infty} \exp\frac{-t^2}{2}\,\mathrm{d}t = \sqrt{2\pi}, \tag{3}$$

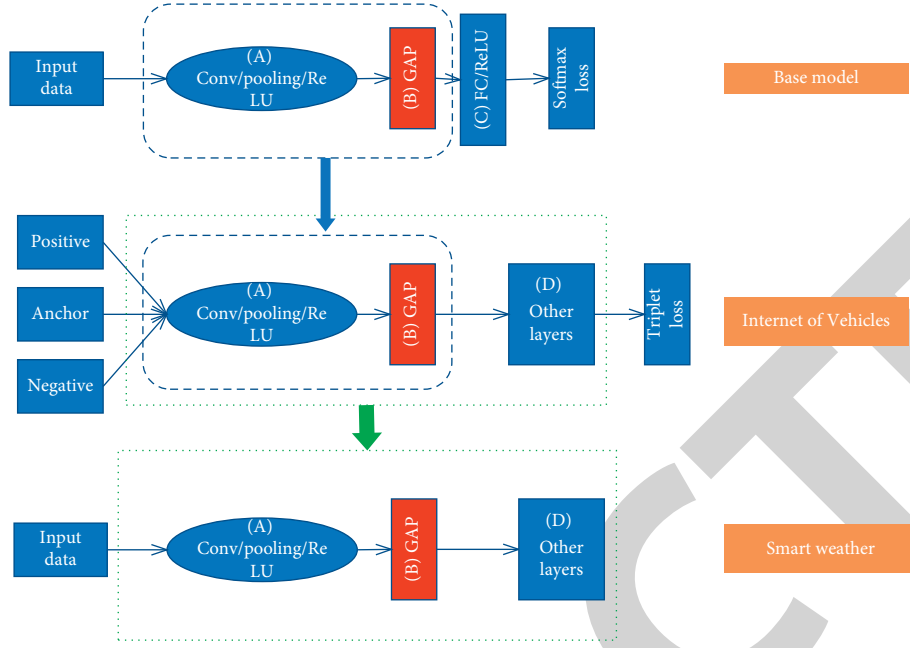the unknown parameter function can be solved.

FIGURE 2: Composition structure diagram of artificial neural networks in smart weather and the Internet of Vehicles.

$$A(x) = \frac{1}{2\pi u \sigma_y \sigma_z}. \tag{4}$$

Under the Gaussian diffusion model of a continuous point source at a high altitude, the pollutant concentration at a certain point is calculated as

$$C(x,y,z) = \frac{q}{2\pi u \sigma_y \sigma_z} \exp\left[-\frac{1}{2}\left(\frac{y^2}{\sigma_y^2} + \frac{z^2}{\sigma_z^2}\right)\right], \tag{5}$$

where u is the wind speed (m/s), q is the pollutant emission (mg/s), σ_y is the standard deviation of plume concentration in horizontal direction, σ_z is standard deviation of plume concentration in vertical direction, σ_y and σ_z are the horizontal and vertical diffusion coefficient; $\sigma_y = 0.146669x^{0.883723}$, $= 0.400167x^{0.632023}$.

According to this diffusion model, the source intensity and wind speed directly affect pollutants' concentration at any point in space [50, 51].

4.2. Diffusion Model of Elevated Point Source

4.2.1. Diffusion Model of Elevated Point Source.
If all the pollutants are reflected after reaching the ground, the "mirror method" is used to solve the real pollution concentration of a specific point. Taking the projection point of the chimney on the ground as the source point o and the coordinates of the effective source point as $(0, 0, H)$, an elevated point source diffusion model is established. The pollution concentration of reference point o is the superposition of the concentration of the real source at $(0, 0, H)$ and the diffusion concentration of the image source at $(0, 0, -H)$. z is the height of the point from the ground [52].

The concentration contribution of the solid source is C_s is

$$C_s = \frac{q}{2\pi u \sigma_y \sigma_z} \exp\left\{-\frac{1}{2}\left[\left(\frac{y^2}{\sigma_y^2} + \frac{(z-H)^2}{\sigma_z^2}\right)\right]\right\}. \tag{6}$$

Image source contribution is

$$C_x = \frac{q}{2\pi u \sigma_y \sigma_z} \exp\left\{-\frac{1}{2}\left[\left(\frac{y^2}{\sigma_y^2} + \frac{(z+H)^2}{\sigma_z^2}\right)\right]\right\}. \tag{7}$$

Add formulas (6) and (7) to get

$$C(x,y,z,H) = \frac{q}{2\pi u \sigma_y \sigma_z} \exp\left(\frac{1}{2}\frac{-y^2}{\sigma_y^2}\right)\left\{\exp\left[\frac{-(z-H)^2}{\sigma_z^2}\right]\right.$$
$$\left. + \exp\left[\frac{-(z-H)^2}{\sigma_z^2}\right]\right\}. \tag{8}$$

If the pollutants are completely absorbed after reaching the ground, the actual diffusion situation should be between the two situations. That is, the concentration value should be between formulas (6) and (8).

4.2.2. Ground Pollutant Concentration.
Compared with the spatial concentration discussed in Section 4.2.1, the concentration of ground pollutants is more closely related to people's lives. The concentration of ground pollutants is equal to the concentration of pollutants in direct contact with human beings. Therefore, based on Section 4.2.1, the concentration of pollutants near the ground can be ignored because of its small distance from the ground. In formula (8),

let $z = 0$, that is, the ground concentration formula is as follows:

$$C(x, y, 0, H) = \frac{q}{\pi u \sigma_y \sigma_z} \left\{ \exp\left[-\frac{1}{2} \left[\frac{y^2}{\sigma_y^2} + \frac{H^2}{\sigma_z^2} \right] \right] \right\}. \tag{9}$$

The concentration distribution along the x-axis is obtained as follows:

$$C(x, 0, 0, H) = \frac{q}{\pi u \sigma_y \sigma_z} \exp\left(-\frac{H^2}{2\sigma_z^2} \right). \tag{10}$$

The concentration in the y direction is normally distributed with the x-axis as the symmetry axis; in the direction along the wind direction, the pollutant concentration first shows an upward trend, and this upward trend continues until a maximum point, then stops increasing, and then continues to decrease to infinity close to 0. In addition, it can also be found that the pollutant concentration is close to 0 when the distance from the emission source is very close. This theory indicates that the pollutant concentration detection device should not be placed too close to the pollution source; otherwise, the detection is invalid [53].

The maximum concentration on the ground and the distance from the source can be derived from formula (9), where C is an arbitrary constant.

$$C_{\max} = \frac{2q}{\pi e u H^2} = \frac{\sigma_y}{\sigma_z} = c. \tag{11}$$

(σ_y/σ_z) formula (10) shows the lager c is, the higher the maximum concentration is; σ_y and σ_z are unknown functions of x, and their value cannot be controlled or expressed concisely. Under the condition that the source intensity remains unchanged, the higher the distance from the pollution source to the ground, the greater the average wind speed and the smaller the maximum concentration on the ground. Generally, when the wind is strong, the concentration of PM2.5 is lower but the wind is a natural force [54, 55]. To reduce the concentration of PM2.5, the height of the pollution source from the ground can be increased as much as possible, such as increasing the length of the exhaust pipe to dilute the concentration of ground pollutants.

4.3. Diffusion Model of Nonpoint Source.

We can treat it as a nonpoint source; that is, according to the spatial distribution characteristics of the point source, it can be divided into square areas with different side lengths of more than 0.5 km for convenient calculation [56]. In this way, the nonpoint source problem can be transformed into the point source problem, and then through the Gaussian diffusion model of the point source, the pollutant concentration at a certain point, that is, formula (10), with the assumption of $2y_0 = 4.3\sigma_{y0}$, σ_{y0}, can be obtained and brought into the formula (10). In this case, H is the average height of the nonpoint source from the ground. Through this formula, we can also conclude that the concentration of pollutants in the space is inversely proportional to the size of H and the size of wind.

In the above assumption, the distribution of pollutants is regarded as on the centroid. In addition, there is another case in which the pollutants are uniformly distributed in the Y direction and diffuse along the arc with a length of $(\pi(x_0 + x)/8)$. Then, the concentration of pollutants at any point of the nonpoint source is calculated by the following formula:

$$C = \sqrt{\frac{2}{\pi}} \frac{q}{u \sigma_z \pi (x_0 + x)/8} \exp\left(-\frac{H}{2\sigma_z^2} \right). \tag{12}$$

4.4. Factors That Affect the Model.

Although this process hinders the diffusion of pollutants in most cases, there are also some problems through these processes in which a reaction produces new pollutants. Here, we assume that the pollutant self-decays with time and the self-settling velocity of particles remains unchanged; then, we can roughly calculate according to the following formula:

$$C(x, y, z, H) = \frac{q}{2\pi u \sigma_y \sigma_z} \exp\left(-\frac{y}{2\sigma_y^2} \right) \left\{ \exp\left[-\frac{(z - H + (u_s x/u))^2}{2\sigma_z^2} \right] + \exp\left[\frac{-(z + H - (u_s x/u))^2}{2\sigma_z^2} \right] \right\} \exp\left(-\frac{0.693x}{Tu} \right), \tag{13}$$

where u_s is the average velocity of particle deposition and T is the average half decay period of pollutants.

5. Analysis and Prediction of PM2.5 Concentration in Beijing, Tianjin, and Hebei

5.1. Impact of Climate Change

5.1.1. Effect of Air Temperature on PM2.5.
The variation range of temperature in the Beijing-Tianjin-Hebei region in a year is generally between −5°C and 40°C. The research object is the meteorological data of the Beijing-Tianjin-Hebei region in 2017. First, the data are processed in two ways: ① the points were removed where the concentration of PM2.5 changes obviously due to the wind force change; ② the points where the concentration of PM2.5 increases or decreases sharply were removed to eliminate the influence of human factors such as artificial rainfall. Figure 3 shows that the trends of the shadow curves of temperature and PM2.5 concentration are roughly the same.

5.1.2. Effect of Relative Humidity on PM2.5.
One of the biggest influencing factors of relative humidity is rainfall, so it is not difficult to find that there is a negative correlation between relative humidity and PM2.5 through data analysis
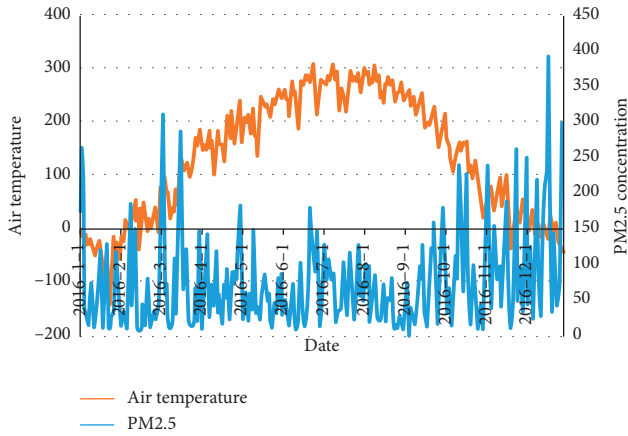
Figure 3: Variation in air temperature/PM2.5 concentration with time.

Figure 4: Relative humidity/PM2.5 concentration versus time.

and image fitting. In fact, this is a good explanation. Relative humidity represents the percentage of water vapor pressure in the air and saturated water vapor pressure at the same temperature. The higher the relative humidity is, the more water molecules there are in the air, which is more conducive to the adsorption of pollutant particles, thus reducing the concentration of PM2.5. Figure 4 shows the relative humidity/PM2.5 concentration versus time.

5.1.3. Influence of Wind on PM2.5. Beijing, Tianjin, and Hebei have warm temperate continental monsoon climates, and the wind speeds on several consecutive days in a certain season are similar. Therefore, when analyzing the influence of wind speed, taking the average PM2.5 concentration over time helps improve the accuracy. Figure 5 shows the variation in the mean wind speed/PM2.5 concentration with time.

Through data analysis, it is not difficult to find that with increasing wind speed, the PM2.5 concentration shows a downward trend. However, there are also fluctuations in the figure that are inconsistent with this trend because the air transported is mixed with pollutants, but generally speaking, the wind force is still negatively correlated with the PM2.5 concentration.

5.2. Impact of Changes in Air Pollutants. PM2.5 refers to fine particles that can be suspended in the air for a long time when their diameter is less than or equal to 2.5 mm in aerodynamics. The chemical composition of PM2.5 mainly includes organic carbon and elemental carbon [42, 43]. The natural source includes sand pollen, which may be mixed with trace amounts of volcanic eruption volcanic ash emitted from the gas. In contrast, the proportion of anthropogenic pollution has increased in recent years [44]. Therefore, this paper focuses on the relationship between these three main air pollutants and PM2.5 concentration changes. Figures 6–8 show the variation in SO_2 (CO, NO_2)/PM2.5 concentration with time.

Through the data fitting image, it is not difficult to find that the changes of SO_2, CO, NO_2, and PM2.5 concentration
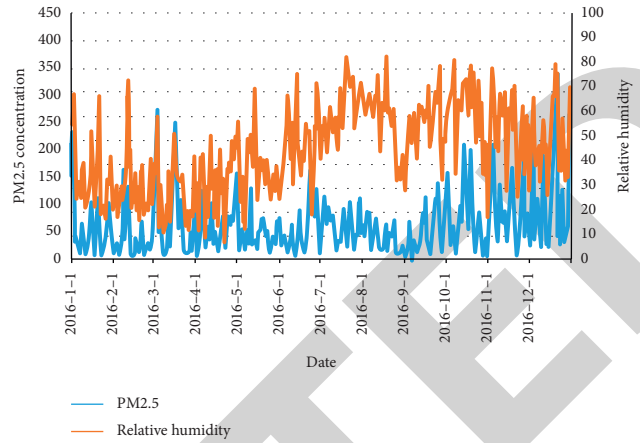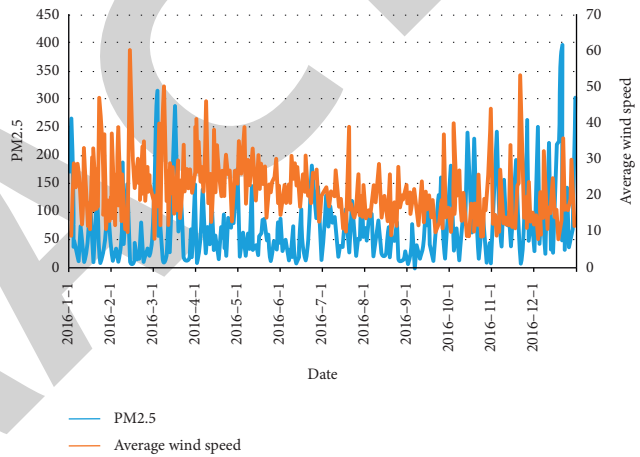

Figure 5: Variation in the mean wind speed/PM2.5 concentration with time.

are generally positively correlated. The higher the pollutant concentration is, the higher the PM2.5 concentration is and the worse the air quality is.

5.3. PM2.5 Concentration Prediction

5.3.1. Beijing PM2.5 Prediction. Figures 9–11 show the MSE of the prediction model error in Beijing, the composite coefficient of the BP neural network in Beijing, and a comparison of the real and predicted PM2.5 concentrations in Beijing.

The minimum output error is 0.014831, and the number of iterations is 32.

5.3.2. Tianjin PM2.5 Prediction. Figures 12–14 show the MSE of the prediction model error in Tianjin, the composite coefficient of the BP neural network in Tianjin, and a comparison of the real and predicted PM2.5 concentrations in Tianjin.

The minimum output error of the BP neural network is 0.046547, and the number of iterations is 3.
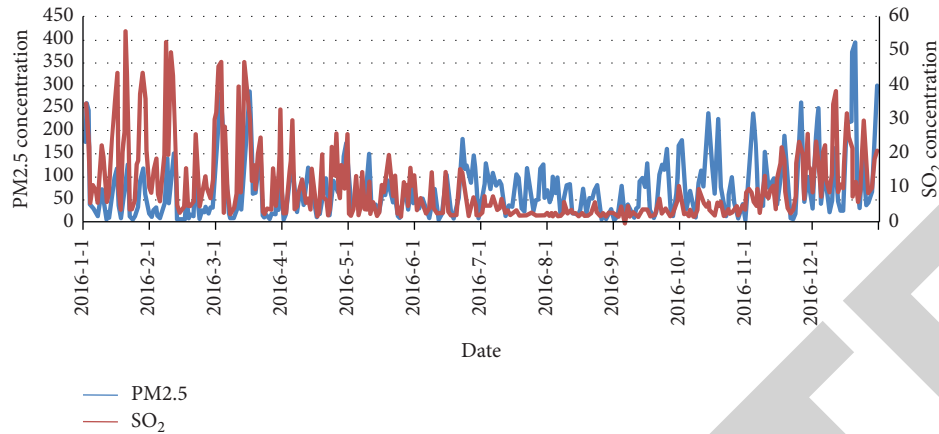
Figure 6: Variation of SO$_2$/PM2.5 concentration with time.

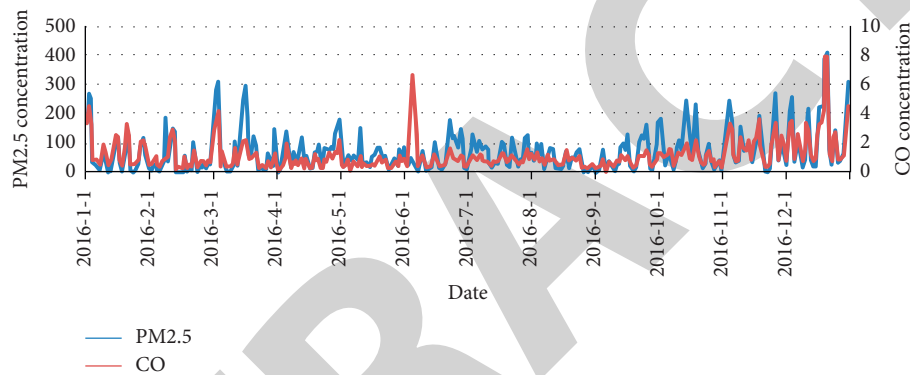Figure 7: Variation of CO/PM2.5 concentration with time.

5.3.3. Shijiazhuang PM2.5 Prediction. Figures 15–17 show the MSE of the prediction model error in Shijiazhuang, the composite coefficient of the BP neural network in Shijiazhuang, and a comparison of the real and predicted PM2.5 concentrations in Shijiazhuang.

The minimum output error of the BP neural network is 0.017496, and the number of iterations is 16.

5.3.4. Experimental Results and Analysis. We use the pollutant emissions from factories in Beijing in 2016 as the data source. According to formula (9), we use several ground concentrations on the *x*-axis (average wind direction) in the elevated point source diffusion model, where the average intensity is not directly given in the data, so we use the product of emission concentration and velocity to replace the average intensity (the result is divided by 3600 to guarantee, and the unit is g/s). The unknown parameters in the formula can be known from the data. The emission concentration and emission rate in the table are average values. The average daily emission concentration comes from the total annual emission concentration divided by 365 days. *C* (mg/m^3) is the concentration value calculated at a distance *x*, the concentration calculated at a distance *x* from point o, and the average wind direction as the positive direction of the *x*-axis.

First, the average daily emission intensity of each pollutant and the pollutant concentration of each test location were calculated according to the average daily emission concentration of each pollutant. Table 1 is the calculation of pollutant concentration.

According to the horizontal comparison of the test results, it can be preliminarily judged that the peak value of the ground concentration is between 50 m and 500 m, and from 500 m to 1000 m, the effect of the increase in the propagation distance on the decrease in the pollutant concentration is very weak. It can be inferred that the concentration continues to drop to infinity close to 0 after the distance is greater than 1000 m.

By establishing the pollutant diffusion model, the simulation of the model can further visualize the diffusion of pollutants. The advantage is that the concentration formula is simplified to the greatest extent by using the mathematically optimal programming method to achieve the greatest degree of simplicity and observation efficiency. However, due to the simplification, many factors with little influence add up after being deleted, thus increasing the error. The biggest problem is that some meteorological factors, such as air pressure, relative humidity, and air temperature, are not considered to influence pollutant diffusion and the random nonuniformity of the pollutant distribution in space. These two points make the
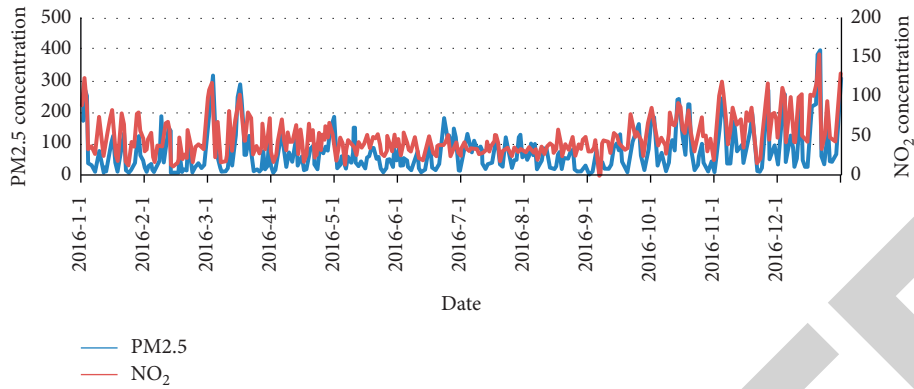
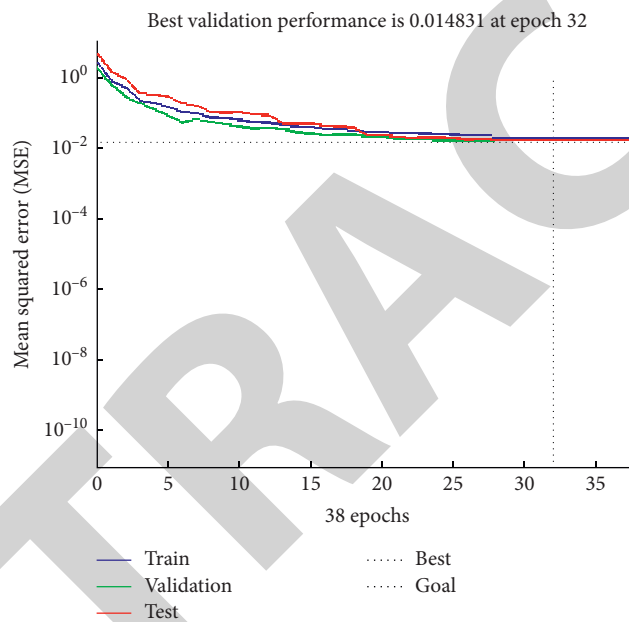Figure 8: Variation of NO$_2$/PM2.5 concentration with time.

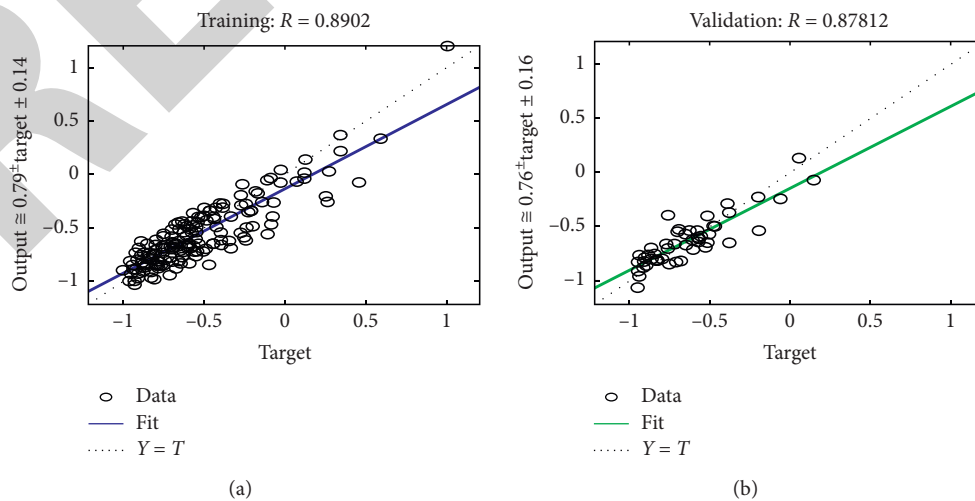Figure 9: MSE of prediction model error in Beijing.

(a)

(b)

Figure 10: Continued.

Test: $R = 0.95539$
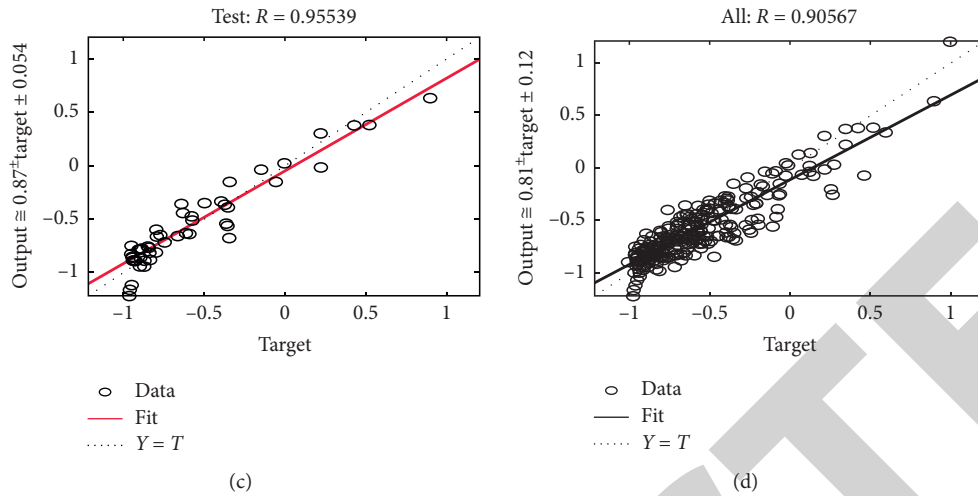
(c)

All: $R = 0.90567$

(d)

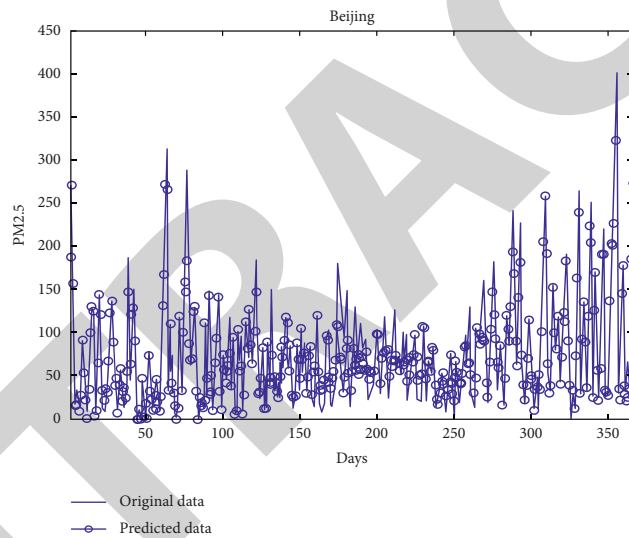Figure 10: Composite coefficient of BP neural network in Beijing.

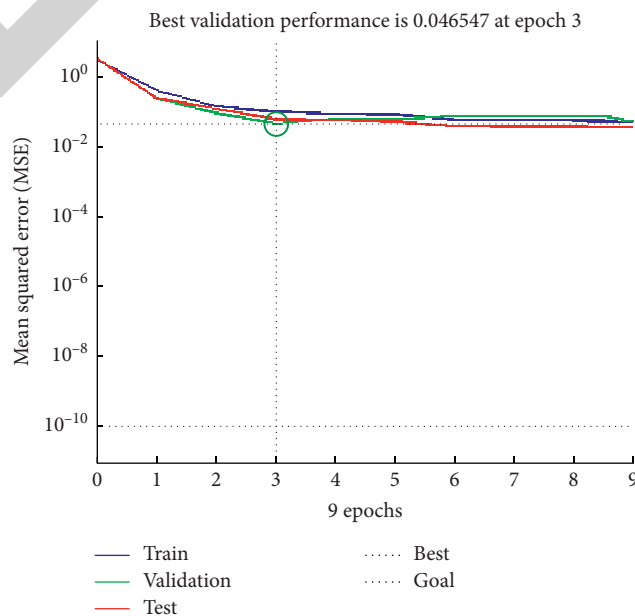Figure 11: Comparison of PM2.5 concentration in Beijing.

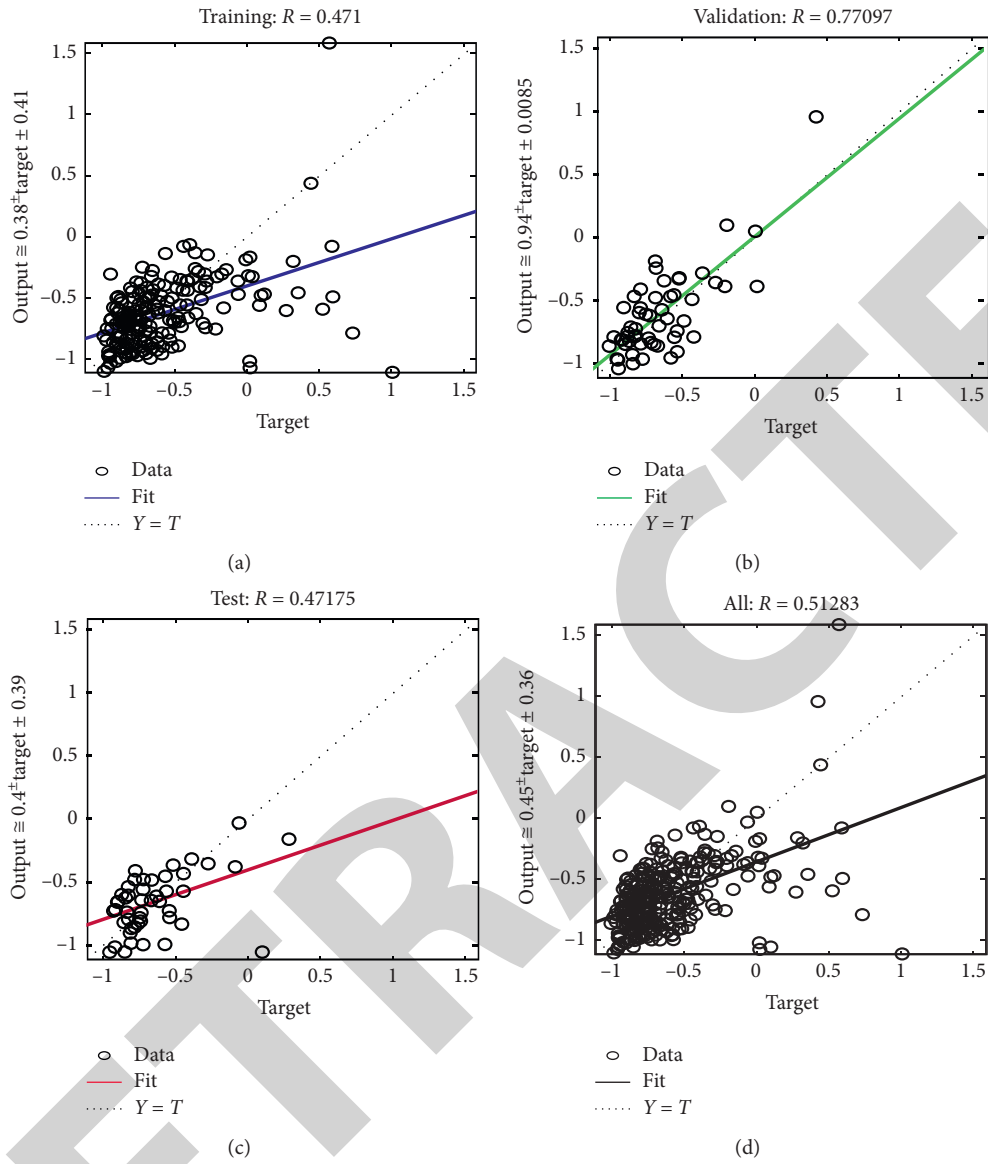Figure 12: MSE of prediction model error in Tianjin.

Figure 13: Composite coefficient of BP neural network in Tianjin.
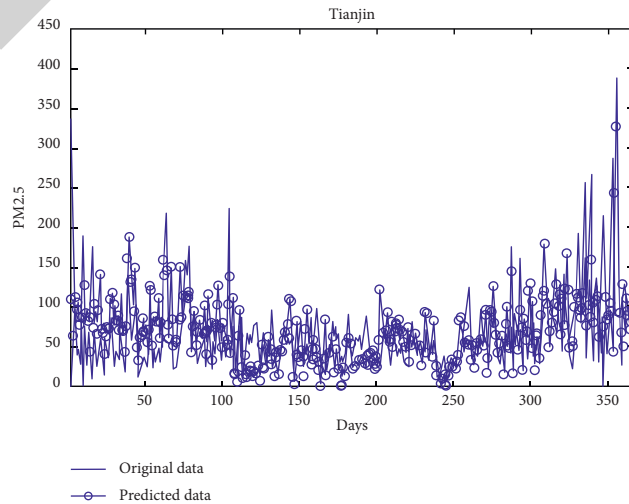

Figure 14: Comparison of PM2.5 concentration in Tianjin.
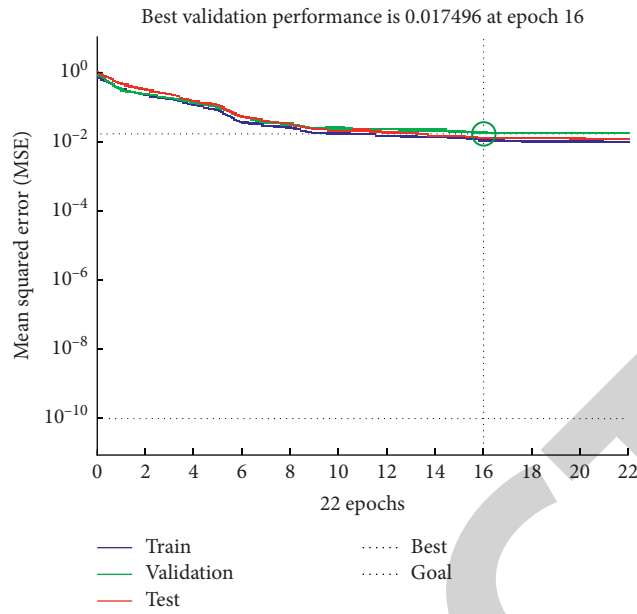
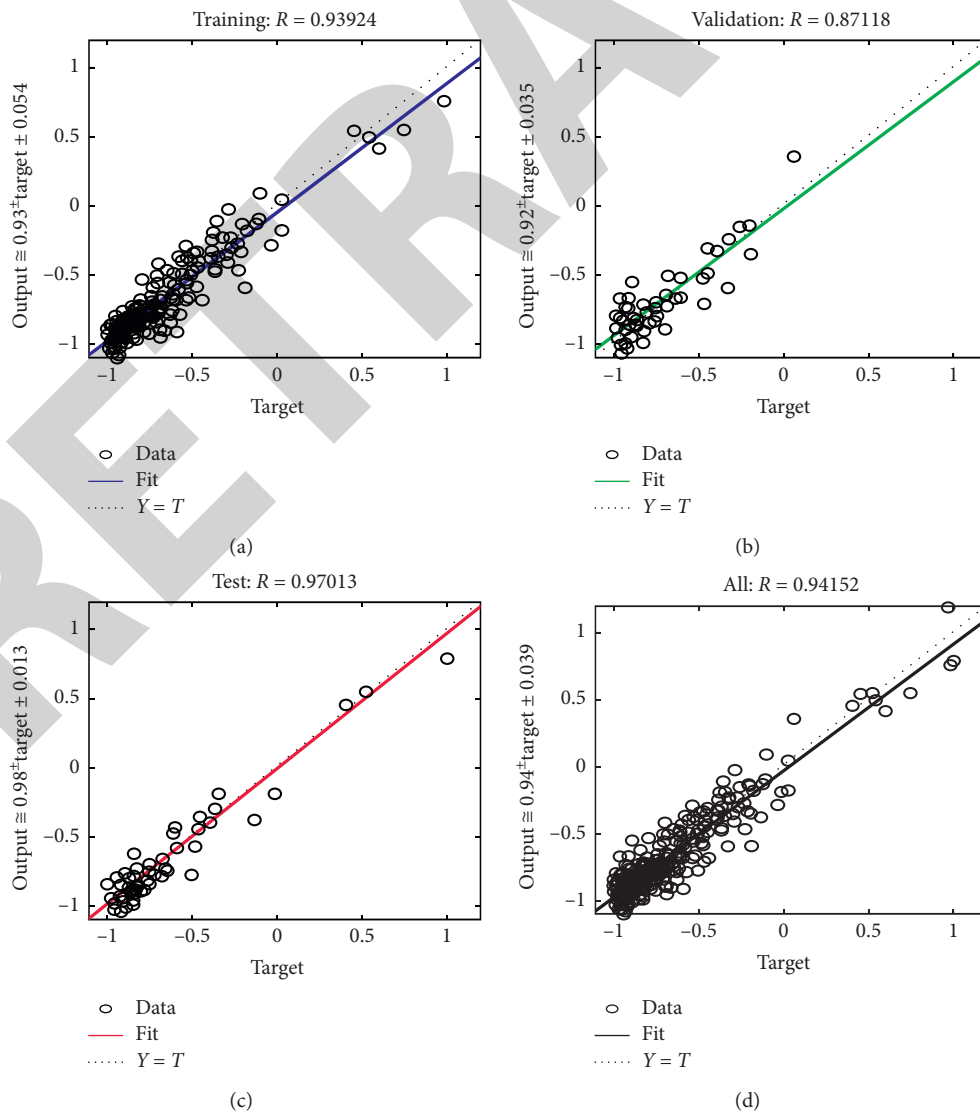FIGURE 15: MSE of prediction model error in Shijiazhuang.

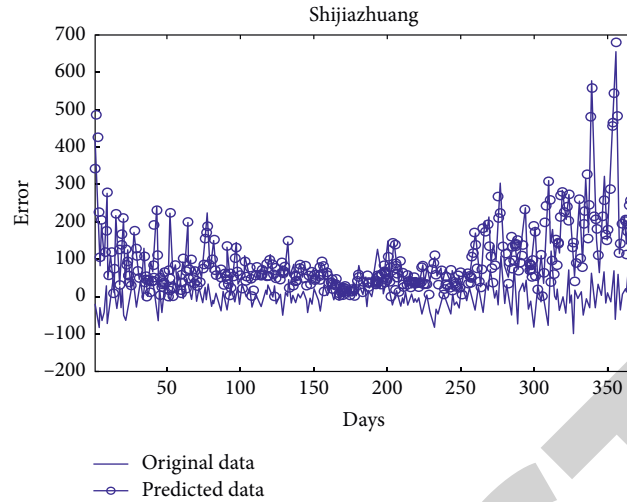FIGURE 16: Composite coefficient of BP neural network in Shijiazhuang.

FIGURE 17: Comparison of PM2.5 concentration in Shijiazhuang.

TABLE 1: Calculation of pollutant concentration.

Pollutant types	Daily average emission concentration (g/m^3)	Discharge rate (m^3/h)	Average strength (g/s)	C (50 m) (mg/m^3)	C (500 m) (mg/m^3)	C (1000 m) (mg/m^3)
BC (black charcoal)	5.8	1100.0	1.77	0.7621	0.0410	$6.06E-52$
CO	690.0	1200.0	230.0	99.0360	5.3286	$7.88E-50$
CO_2	1324.7	2500.0	919.9	396.1008	21.3121	$3.15E-49$
NH_3	68.6	1100.0	21.0	9.0424	0.4865	$7.20E-51$
OC (organic carbon)	4.8	1100.0	1.47	0.6330	0.0341	$5.04E-52$
VOC (volatile organic compounds)	895.8	3200.0	796.3	342.8797	18.4485	$2.73E-49$
PMC	19.6	2700.0	14.7	6.3297	0.3406	$5.04E-51$
SO_2	41.0	2300.0	26.2	11.2815	0.6070	$8.98E-51$
NO_x (nitrogen oxide)	450.0	1200.0	150.0	64.5887	3.4752	$5.14E-50$
$PM_{2.5}$	46.69	2700.0	35.0	15.0707	0.8109	$1.20E-50$

environment more readable. The final model produces some errors, and the control and distribution of pollutants are unreasonable.

6. Conclusion and Future Work

The Internet of Vehicles industry has entered a stage of rapid development. At present, the security functions and measures of the whole industry still need to be improved, and there is still a large space to improve the in-depth services for people, vehicles, roads, facilities, networks, and other comprehensive scenarios. Thus, the impact of weather on traffic safety and operational efficiency can be seen. In the development process of the Internet of Vehicles, meteorological services are an indispensable part. As a planet suspended in the universe, the main way for the Earth to exchange energy with the outside world is through radiation. By receiving the sun's radiation and emitting infrared radiation simultaneously, the Earth finally achieves a dynamic equilibrium state. In this paper, through the haze prediction model established by a neural network and the pollutant diffusion model, we can preliminarily determine the PM2.5 concentration of the day according to the daily meteorological factors and pollutant concentration and obtain the concentration distribution of different regions in the space under the premise of free diffusion and a single pollution source.

Data Availability

The data used to support the findings of this study are available from the corresponding author upon request.

Conflicts of Interest

The authors declare that they have no conflicts of interest.

Acknowledgments

References

[1] Y. Yang, M. Chen, X. Zhao et al., "Impacts of aerosol-radiation interaction on meteorological forecasts over northern China by offline coupling of the WRF-chem-simulated aerosol optical depth into WRF: a case study during a heavy pollution event," *Atmospheric Chemistry and Physics*, vol. 20, no. 21, pp. 12527–12547, 2020.

[2] Y. Chen, W. Zheng, W. Li, and Y. Huang, "Large group activity security risk assessment and risk early warning based on random forest algorithm," *Pattern Recognition Letters*, vol. 144, pp. 1–5, 2021.

[3] K. Zhang, J. Zhang, X. Ma et al., "History matching of naturally fractured reservoirs using a deep sparse autoencoder," *SPE Journal*, pp. 1–22, 2021.

[4] C. Zhao and J. Li, "Equilibrium selection under the Bayes-based strategy updating rules," *Symmetry*, vol. 12, no. 5, pp. 1–11, 2020.

[5] P. Han, H. Zhou, and B. Zhou, "Principle research and implementation of BP neural network," *Radio and Television Information*, vol. 21, no. 10, pp. 121–125, 2018.

[6] Q. Xie, "Partial application experience of artificial neural network in medical image processing," *Image Research and Medical Application*, vol. 2, no. 15, pp. 228-229, 2018.

[7] C. Yang, F. Gao, and M. Dong, "Energy efficiency modeling of integrated energy system in coastal areas," *Journal of Coastal Research*, vol. 103, no. SI, pp. 995–1001, 2020.

[8] Y. Zhou, L. Tian, C. Zhu, X. Jin, and Y. Sun, "Video coding optimization for virtual reality 360-degree source," *IEEE Journal of Selected Topics in Signal Processing*, vol. 14, no. 1, pp. 118–129, 2020.

[9] H. Zhang, Y. Tian, and B. Liu, "Spatial temporal characteristics and cluster analysis of chemical components for ambient PM2.5 in Wuhan," *Huanjing Kexue*, vol. 40, no. 11, pp. 4764–4773, 2019.

[10] X. Ma, T. Sha, J. Wang, H. Jia, and R. Tian, "Investigating impact of emission inventories on PM2.5 simulations over north China plain by WRF-chem," *Atmospheric Environment*, vol. 195, pp. 125–140, 2018.

[11] L. Chen, Y. Gao, and M. Zhang, "MICS-Asia III: multi-model comparison and evaluation of aerosol over east Asia," *Atmospheric Chemistry and Physics*, vol. 19, no. 18, pp. 11911–11937, 2019, þ.

[12] L. He, J. Shen, and Y. Zhang, "Ecological vulnerability assessment for ecological conservation and environmental management," *Journal of Environmental Management*, vol. 206, no. 1, pp. 1115–1125, 2018.

[13] J. Shen and Q. Xu, "Prediction of shear strength of RCC dam surface by artificial neural network and fuzzy logic system," *Journal of Tsinghua University (Natural Science Edition)*, vol. 59, no. 5, pp. 345–353, 2019.

[14] H. Hua, S. Jiang, H. Sheng et al., "A high spatial-temporal resolution emission inventory of multi-type air pollutants for Wuxi city," *Journal of Cleaner Production*, vol. 229, pp. 278–288, 2019.

[15] J. Zhao, J. Liu, J. Jiang, and F. Gao, "Efficient deployment with geometric analysis for mmWave UAV communications," *IEEE Wireless Communications Letters*, vol. 9, no. 7, pp. 1115–1119, 2020.

[16] Q. Jiang, F. Shao, W. Lin, K. Gu, G. Jiang, and H. Sun, "Optimizing multistage discriminative dictionaries for blind image quality assessment," *IEEE Transactions on Multimedia*, vol. 20, no. 8, pp. 2035–2048, 2018.

[17] C. Zuo, J. Sun, J. Li, J. Zhang, A. Asundi, and Q. Chen, "High-resolution transport-of-intensity quantitative phase microscopy with annular illumination," *Scientific Reports*, vol. 7, no. 1, pp. 7622–7654, 2017.

[18] H. Ke, S. Gong, J. He, C. Zhou, L. Zhang, and Y. Zhou, "Spatial and temporal distribution of open bio-mass burning in China from 2013 to 2017," *Atmospheric Environment*, vol. 210, pp. 156–165, 2019.

[19] K. M. Mok and S. C. Tam, "Short-term prediction of SO_2 concentration in Macau with artificial neural networks," *Energy & Buildings*, vol. 28, no. 3, 1998.

[20] Y. Yang, Y. Li, J. Yao et al., "Dynamic pore-scale dissolution by CO_2-saturated brine in carbonates: impact of homogeneous versus fractured versus vuggy pore structure," *Water Resources Research*, vol. 56, no. 4, 2020.

[21] P. Perez and G. Salini, "PM2.5 forecasting in a large city: comparison of three methods," *Atmospheric Environment*, vol. 42, no. 35, pp. 1347–1363, 2008.

[22] F. Yin, X. Xue, C. Zhang et al., "Multifidelity genetic transfer: an efficient framework for production optimization," *SPE Journal*, pp. 1–22, 2021.

[23] L. Zhang, J. Zheng, S. Tian et al., "Effects of Al^{3+} on the microstructure and bioflocculation of anoxic sludge," *Journal of Environmental Sciences*, vol. 91, no. 5, pp. 212–221, 2020.

[24] R. Liu, Z. Han, and J. Li, "Analysis of meteorological characteristics of winter haze events in Beijing," *Climate and Environment Research*, vol. 19, no. 2, pp. 164–172, 2014.

[25] C. Liu, X. Deng, J. Liu, T. Peng, S. Yang, and Z. Zheng, "Dynamic response of saddle membrane structure under hail impact," *Engineering Structures*, vol. 214, Article ID 110597, 2020.

[26] L. Ding, L. Huang, S. Li et al., "Definition and application of variable resistance coefficient for wheeled mobile robots on deformable terrain," *IEEE Transactions on Robotics*, vol. 36, no. 3, pp. 894–909, 2020.

[27] R. Prasad and K. D. Yadav, "Use of response surface methodology and artificial neural network approach for methylene blue removal by adsorption onto water hyacinth," *Water Conservation and Management*, vol. 4, no. 2, pp. 83–89, 2021.

[28] S. Feng, H. Lu, P. Tian et al., "Analysis of microplastics in a remote region of the Tibetan Plateau: implications for natural environmental response to human activities," *Science of The Total Environment*, vol. 739, no. 12, 2020.

[29] S.-J. Lu, D. Wang, Z. Wang et al., "Investigating the role of meteorological factors in the vertical variation in PM2.5 by unmanned aerial vehicle measurement," *Aerosol and Air Quality Research*, vol. 19, no. 7, pp. 1493–1507, 2019.

[30] C. Zuo, Q. Chen, L. Tian, L. Waller, and A. Asundi, "Transport of intensity phase retrieval and computational imaging for partially coherent fields: the phase space perspective," *Optics and Lasers in Engineering*, vol. 71, no. 8, pp. 20–32, 2015.

[31] W. Chen, Y. Liu, and X. Wu, "Spatial and temporal characteristics of air quality and cause analysis of heavy pollution in northeast China," *Huanjing Kexue*, vol. 40, no. 11, pp. 4810–4823, 2019.

[32] W. Zhang, Y. Hu, J. Liu et al., "Progress of ethylene action mechanism and its application on plant type formation in crops," *Saudi Journal of Biological Sciences*, vol. 27, no. 6, pp. 1667–1673, 2020.

[33] Y. Xie, Y. Xue, J. Guang et al., "Deriving a global and hourly data set of aerosol optical depth over land using data from four geostationary satellites: GOES-16, MSG-1, MSG-4, and Himawari-8," *IEEE Transactions on Geoscience and Remote Sensing*, vol. 58, no. 3, pp. 1538–1549, 2020.

[34] H. Feng, Z. Feng, and H. Feng, "One new method of PM2.5 concentration inversion based on difference index," *Spectroscopy and Spectral Analysis*, vol. 38, no. 10, pp. 3012–3016, 2018.

[35] S. Lu, S. Gong, and J. He, "Uncertainty analysis of spatiotemporal characteristics of haze pollution from 1961 to 2017 in China," *Atmospheric Pollution Research*, vol. 11, no. 2, pp. 310–318, 2020.

[36] X. Wu, T. V. Vu, Z. Shi, R. M. Harrison, D. Liu, and K. Cen, "Characterization and source apportionment of carbonaceous $PM_{2.5}$ particles in China—a review," *Atmospheric Environment*, vol. 189, pp. 187–212, 2018.

[37] S. P. Parajuli and C. S. Zender, "Projected changes in dust emissions and regional air quality due to the shrinking Salton Sea," *Aeolian Research*, vol. 33, pp. 82–92, 2018.

[38] X. Chen, Z. Wang, J. Li et al., "Explaining the spatiotemporal variation of fine particle number concentrations over Beijing and surrounding areas in an air quality model with aerosol microphysics," *Environmental Pollution*, vol. 231, pp. 1302–1313, 2017.

[39] A. Li, D. Spano, J. Krivochiza et al., "A tutorial on interference exploitation via symbol-level precoding: overview, state-of-the-art and future directions," *IEEE Communications Surveys & Tutorials*, vol. 22, no. 2, pp. 796–839, 2020.

[40] L. He, F. Shao, and L. Ren, "Sustainability appraisal of desired contaminated groundwater remediation strategies: an information-entropy-based stochastic multi-criteria preference model," *Environment, Development and Sustainability*, vol. 23, no. 2, 2021.

[41] C. Jiang, R. Li, T. Chen, C. Xu, L. Li, and S. Li, "A two-lane mixed traffic flow model with drivers' intention to change lane based on cellular automata," *International Journal of Bio-Inspired Computation*, vol. 16, no. 4, pp. 229–240, 2020.

[42] Z. Liu, L. Lang, B. Hu, L. Shi, B. Huang, and Y. Zhao, "Emission reduction decision of agricultural supply chain considering carbon tax and investment cooperation," *Journal of Cleaner Production*, vol. 294, no. 4, Article ID 126305, 2021.

[43] B. Bai, Z. Guo, C. Zhou, W. Zhang, and J. Zhang, "Application of adaptive reliability importance sampling-based extended domain PSO on single mode failure in reliability engineering," *Information Sciences*, vol. 546, pp. 42–59, 2021.

[44] J. Xu, R. Rahmatizadeh, L. Bölöni, and D. Turgut, "Real-time prediction of taxi demand using recurrent neural networks," *IEEE Transactions on Intelligent Transportation Systems*, vol. 19, no. 8, pp. 2572–2581, 2018.

[45] A. Nema, K. D. Yadav, and R. A. Christian, "Effect of retention time on primary media for greywater treatment," *Water Conservation and Management*, vol. 1, no. 1, pp. 1–3, 2017.

[46] J. Liu, Y. Liu, and X. Wang, "An environmental assessment model of construction and demolition waste based on system dynamics: a case study in Guangzhou," *Environmental Science and Pollution Research*, vol. 27, no. 30, pp. 37237–37259, 2020.

[47] J. Liu, Y. Yi, and X. Wang, "Exploring factors influencing construction waste reduction: a structural equation modeling approach," *Journal of Cleaner Production*, vol. 276, no. 12, pp. 1–33, 2020.

[48] X. Xue, K. Zhang, K. C. Tan et al., "Affine transformation-enhanced multifactorial optimization for heterogeneous problems," *IEEE Transactions on Cybernetics*, pp. 1–15, 2020.

[49] H. Zhang, M. Sun, L. Song, J. Guo, and L. Zhang, "Fate of NaClO and membrane foulants during in-situ cleaning of membrane bioreactors: combined effect on thermodynamic properties of sludge," *Biochemical Engineering Journal*, vol. 147, no. 7, pp. 146–152, 2019.

[50] M. Sun, L. Yan, L. Zhang, L. Song, J. Guo, and H. Zhang, "New insights into the rapid formation of initial membrane fouling after in-situ cleaning in a membrane bioreactor," *Process Biochemistry*, vol. 78, no. 3, pp. 108–113, 2019.

[51] Z. Wu, J. Cao, Y. Wang, Y. Wang, L. Zhang, and J. Wu, "hPSD: a hybrid PU-learning-based spammer detection model for product reviews," *IEEE Transactions On Cybernetics*, vol. 50, no. 4, pp. 1595–1606, 2018.

[52] X. C. Hong, G. Y. Wang, J. Liu, L. Song, and E. T. Wu, "Modeling the impact of soundscape drivers on perceived birdsongs in urban forests," *Journal of Cleaner Production*, vol. 292, Article ID 125315, 2021.

[53] L. Zhang, M. Zhang, S. You, D. Ma, J. Zhao, and Z. Chen, "Effect of Fe^{3+} on the sludge properties and microbial community structure in a lab-scale A^2O process," *Science of The Total Environment*, vol. 780, no. 8, pp. 1–10, 2021.

[54] H. O. Nwankwoala, M. T. Harry, and T. Warmate, "Assessing aquifer vulnerability and contaminant plume at artisanal refining sites in parts of Okrika and Ogu-Bolo local government areas, Rivers state, Nigeria," *Water Conservation and Management*, vol. 4, no. 2, pp. 58–62, 2020.

[55] M. Zhang, J. Montewka, T. Manderbacka, P. Kujala, and S. Hirdaris, "A big data analytics method for the evaluation of ship-ship collision risk reflecting hydrometeorological conditions," *Reliability Engineering & System Safety*, vol. 213, Article ID 107674, 2021.

[56] Q. Yue and L. Zhang, "Two-sided matching for hesitant fuzzy numbers in smart intelligent technique transfer," *Mechanical Systems and Signal Processing*, vol. 139, Article ID 106643, 2020.